Supporting Information

Strong direct-bandgap photoluminescence of suspended few-layer MoS_2 via interlayer decoupling

Jiahao Wu[1], *Jinyan Huang*[2], *Juncong She*[1,*], *and Shasha Li*[2,*]

[1]State Key Laboratory of Optoelectronic Materials and Technologies, Guangdong Province Key Laboratory of Display Material and Technology, School of Electronics and Information Technology, Sun Yat-sen University, Guangzhou 510275, People's Republic of China

[2]School of Integrated Circuits, Sun Yat-sen University, Shenzhen 518107, People's Republic of China

*Email: lishsh89@mail.sysu.edu.cn; shejc@mail.sysu.edu.cn

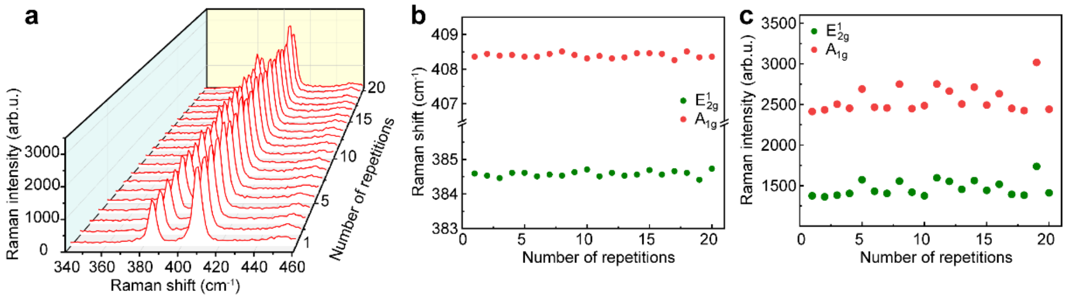

Figure S1. Raman measurements of MoS_2. (a) Raman spectra of MoS_2 obtained with a laser power of 6 μW. The exposure time of each measurement is 10 s. (b) Raman shifts of the E^1_{2g} and A_{1g} peaks. (c) Raman intensities of the E^1_{2g} and A_{1g} peaks. It can be seen that the Raman measurements maintain good repeatability over multiple measurements. The results suggest that the structural quality of the tested MoS_2 samples can be well maintained after the optical measurements with such a low power.

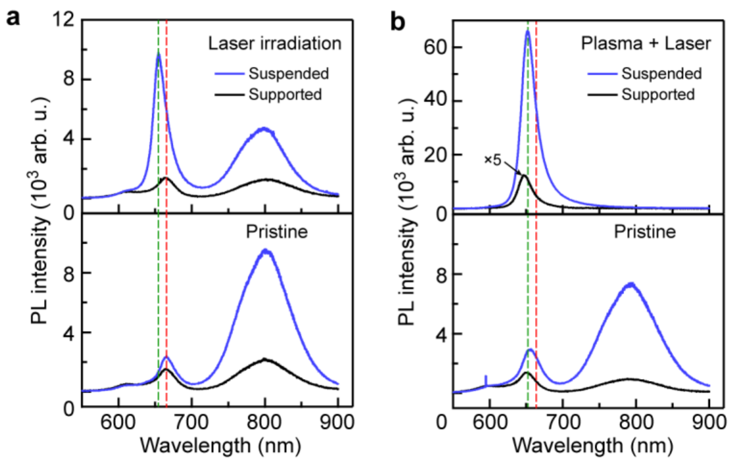

Figure S2. Enhanced radiative emission of A excitons. (a) PL spectra from both suspended and supported regions of MoS_2 before (bottom) and after (top) laser irradiation. (b) PL spectra from MoS_2 before (bottom) and after (top) the combined plasma and laser treatment. The green and red dashed line indicate the positions of A excitons (~654 nm) and trions (~663 nm) extracted from Guassian fitting. The asprepared MoS_2 flake for laser treatment was highly n-doped, which dominated the emission spectrum and made the A exciton peak nearly indistinguishable. Following laser irradiation, a pronounced enhancement of the A exciton emission was observed, indicating a significant reduction in electron doping. A similar enhancement, accompanied by the complete suppression of indirect bandgap emission, was also achieved with the combined plasma and laser treatment.

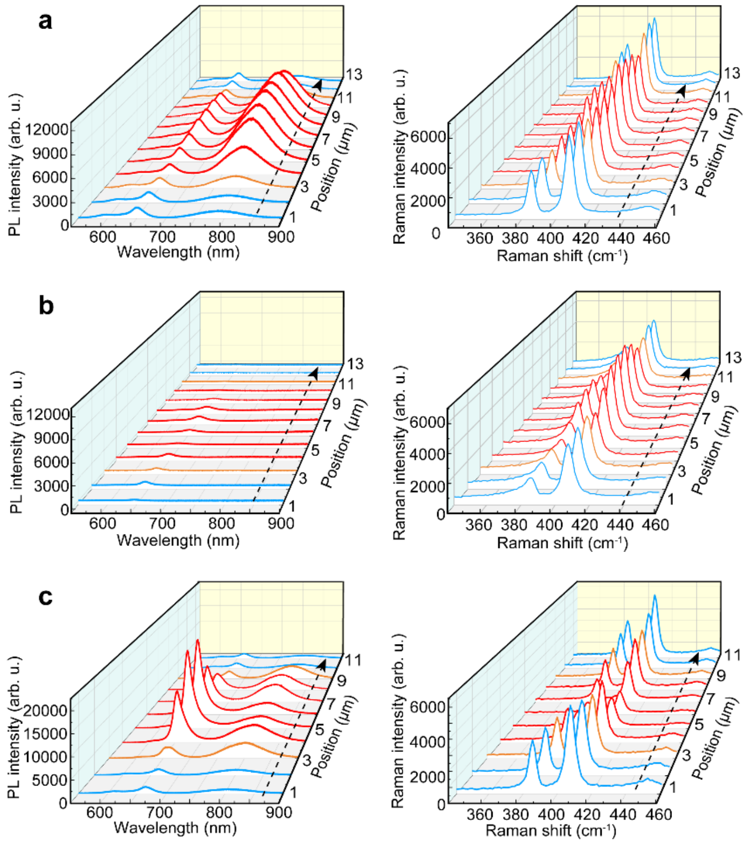

Figure S3. Optical characterizations. (a–c) PL and Raman spectra of the pristine bilayer MoS_2 (a), plasma-treated bilayer MoS_2 (b), and laser-treated bilayer MoS_2 (c). The PL and Raman spectra are shown in the left and right panels, respectively.

Table S1 Average values and standard deviations of Raman peak frequencies and their difference for different types of MoS_2 samples.

MoS_2 sample	ω_E (cm^{-1})	ω_A (cm^{-1})	$\Delta\omega$(cm^{-1})
Pristine 1L	385.94 ± 0.14	405.91 ± 0.05	19.97 ± 0.28
Pristine sus 1L	385.99 ± 0.24	405.98 ± 0.20	19.99 ± 0.18
Pristine 2L	385.63 ± 0.11	407.89 ± 0.04	22.26 ± 0.13
Pristine sus 2L	385.28 ± 0.03	407.67 ± 0.05	22.39 ± 0.04
Plasma 2L	385.61 ± 0.13	407.65 ± 0.05	22.04 ± 0.15
Plasma sus 2L	384.98 ± 0.16	407.37 ± 0.10	22.39 ± 0.12
Laser 2L	385.64 ± 0.07	407.94 ± 0.07	22.3 ± 0.10
Laser sus 2L	385.40 ± 0.19	407.88 ± 0.10	22.48 ± 0.20
(Plasma + laser) 2L	385.94 ± 0.14	408.06 ± 0.05	22.12 ± 0.16
(Plasma + laser) sus 2L	386.20 ± 0.24	406.66 ± 0.20	20.46 ± 0.34

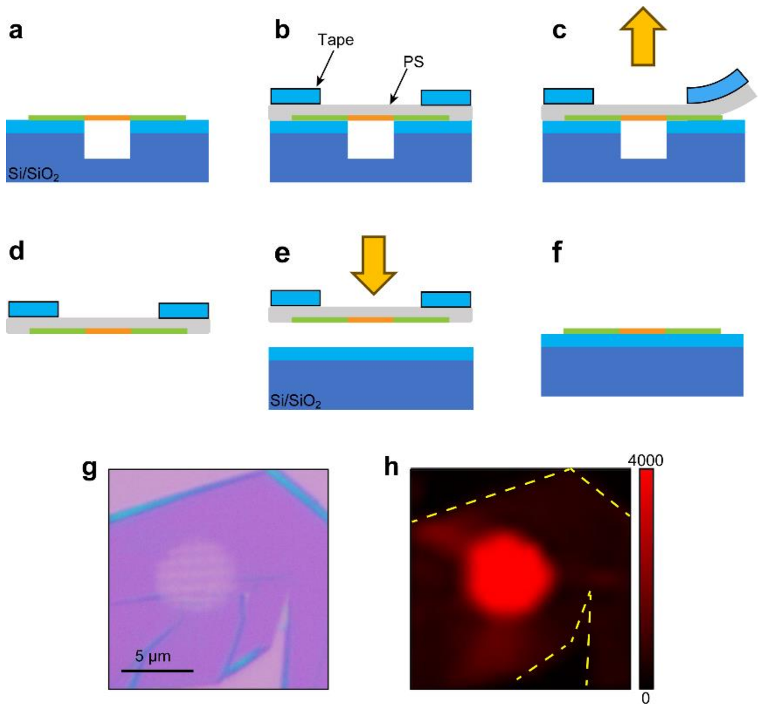

Figure S4 Transfer process. (a) The treated MoS_2 sample on the Si/SiO_2 substrate with micro-holes. (b) The MoS_2 sample was spin-coated with the polystyrene (PS) solution, forming a PS film after drying in air. (c) The PS film was exfoliated by tape with the MoS_2 sample attached on the PS film. (d–f) The PS film was transferred to a bare

Si/SiO_2 substrate and removed by toluene solution, leaving the MoS_2 sample on the substrate. (g,h) Optical microscopy (g) and PL mapping (h) images of the treated MoS_2 transferred from the hole region to a bare Si/SiO_2 substrate.

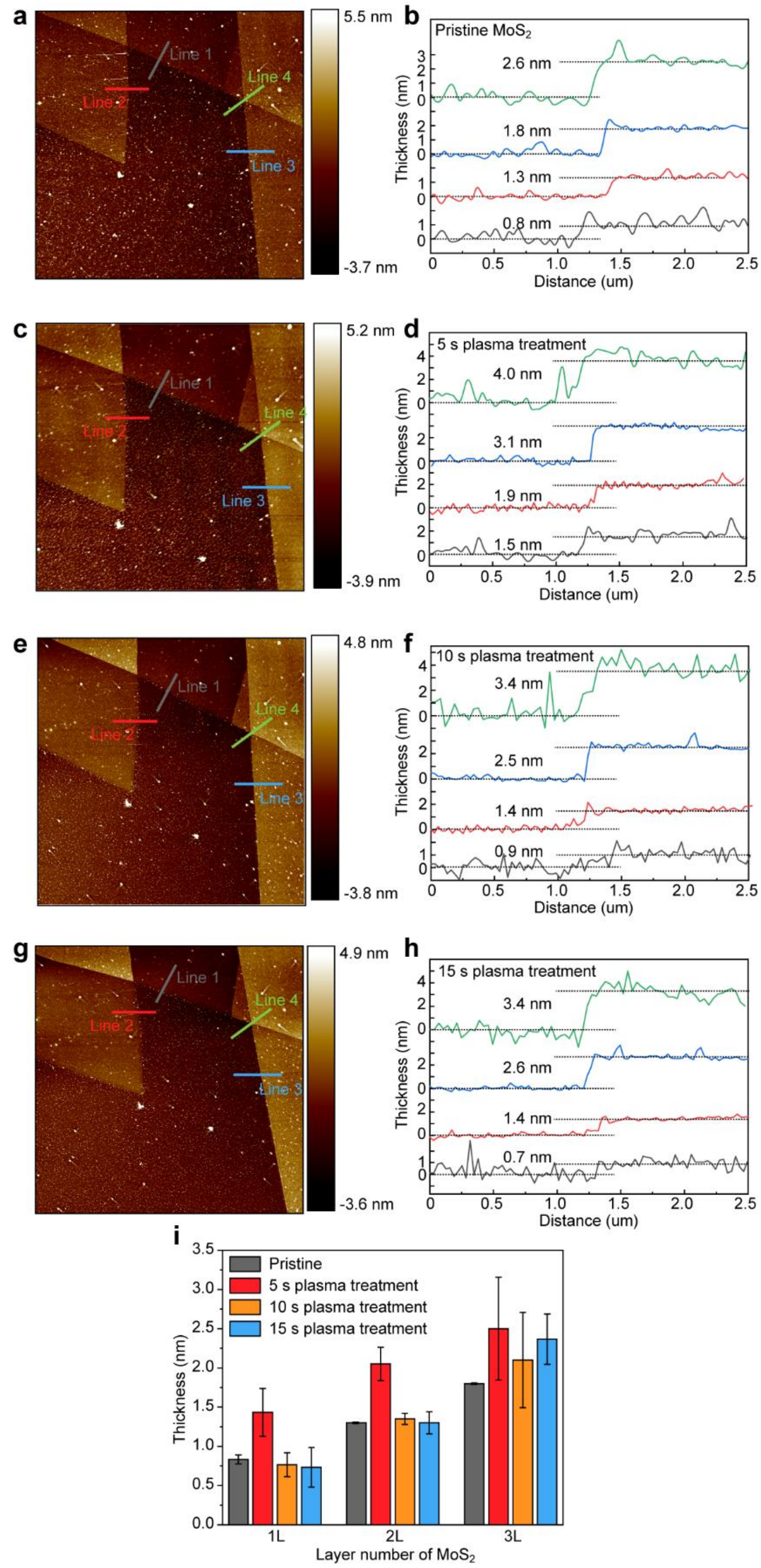

Figure S5 AFM characterization of plasma-treated MoS_2. (a,b) AFM image (a) of the pristine MoS_2 and height profiles (b) along the lines in (a). (c–h) AFM images and corresponding height profiles obtained from the MoS_2 samples after plasma treatments for 5 s (c,d), 10 s (e,f), and 15 s (g,h). (i) Histogram summarizing the thickness variations of the MoS_2 samples after plasma treatments.

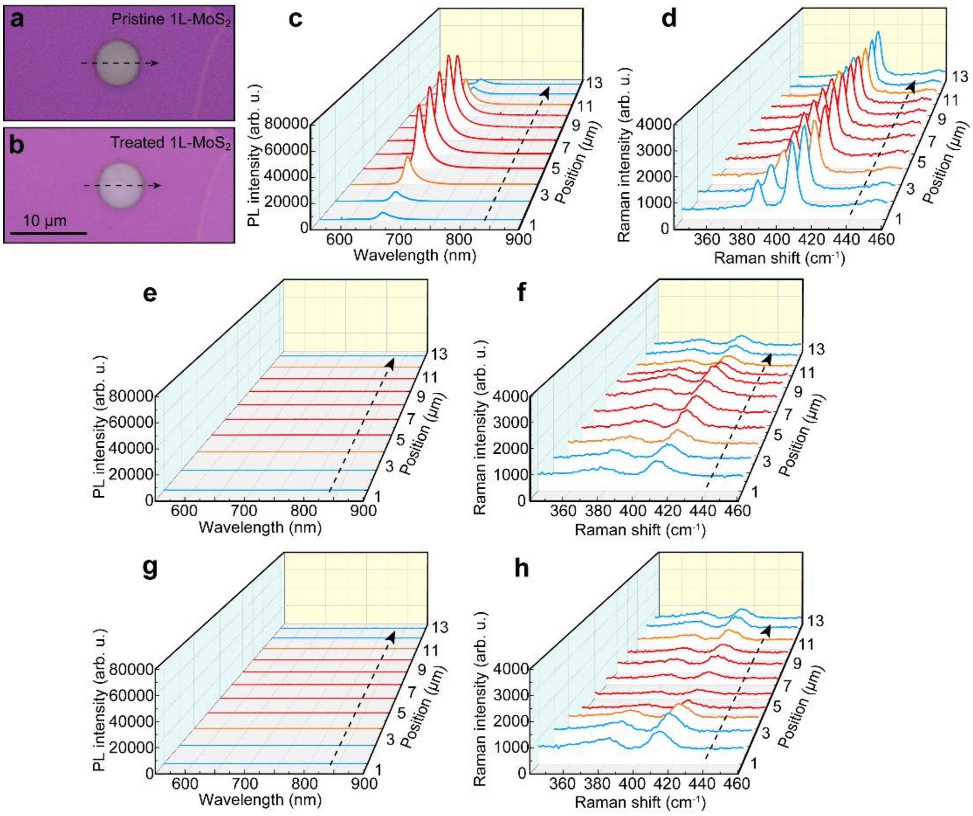

Figure S6 Optical characterizations on the monolayer MoS_2. (a, b) Optical microscopy images of monolayer MoS_2 before (a) and after (b) the plasma and laser treatments. (c, d) PL (c) and Raman (d) spectra of the pristine monolayer MoS_2 sample. The PL emission of suspended monolayer MoS_2 is significantly stronger than that of the supported one, which is consistent with other studies.[1,2] The Raman spectra of pristine monolayer MoS_2 show no obvious difference in the suspended and supported region. Here, Raman peaks corresponding to the A'_1 and E'_1 modes of monolayer MoS_2 due to D_{3h} point group are provided.[3] (e, f) PL and Raman spectra of the plasma-treated monolayer MoS_2 sample. (g, h) PL and Raman spectra of the monolayer MoS_2 after plasma treatment followed by laser irradiation.

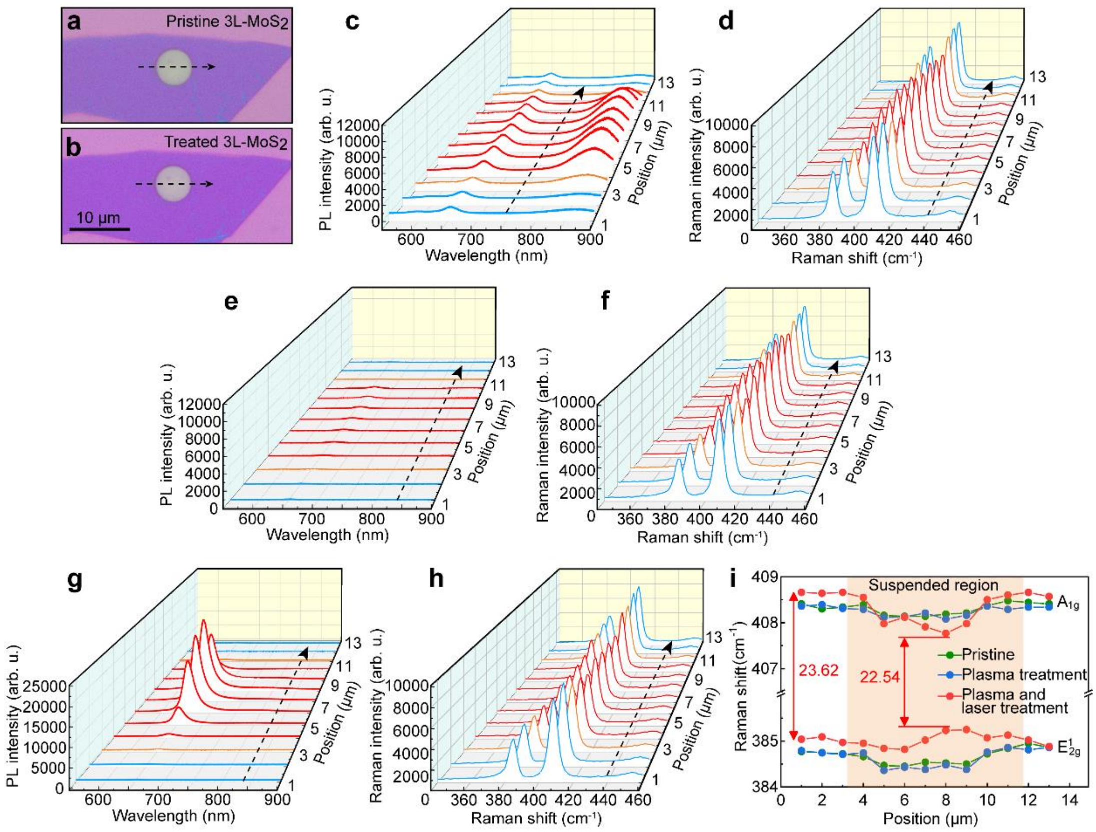

Figure S7. Optical characterizations on the trilayer MoS_2. (a, b) Optical microscopy images of trilayer MoS_2 before (a) and after (b) the plasma and laser treatments. (c, d) PL (c) and Raman (d) spectra of the pristine trilayer MoS_2 sample. (e, f) PL and Raman spectra of the plasma-treated trilayer MoS_2 sample. (g, h) PL and Raman spectra of the trilayer MoS_2 after plasma treatment followed by laser irradiation. (i) Raman shifts of the E′1 and A′1 modes obtained from different types of MoS_2 samples. The wavenumber difference of the two dominant Raman modes decreased after the plasma and laser treatments, suggesting the emergence of interlayer decoupling.

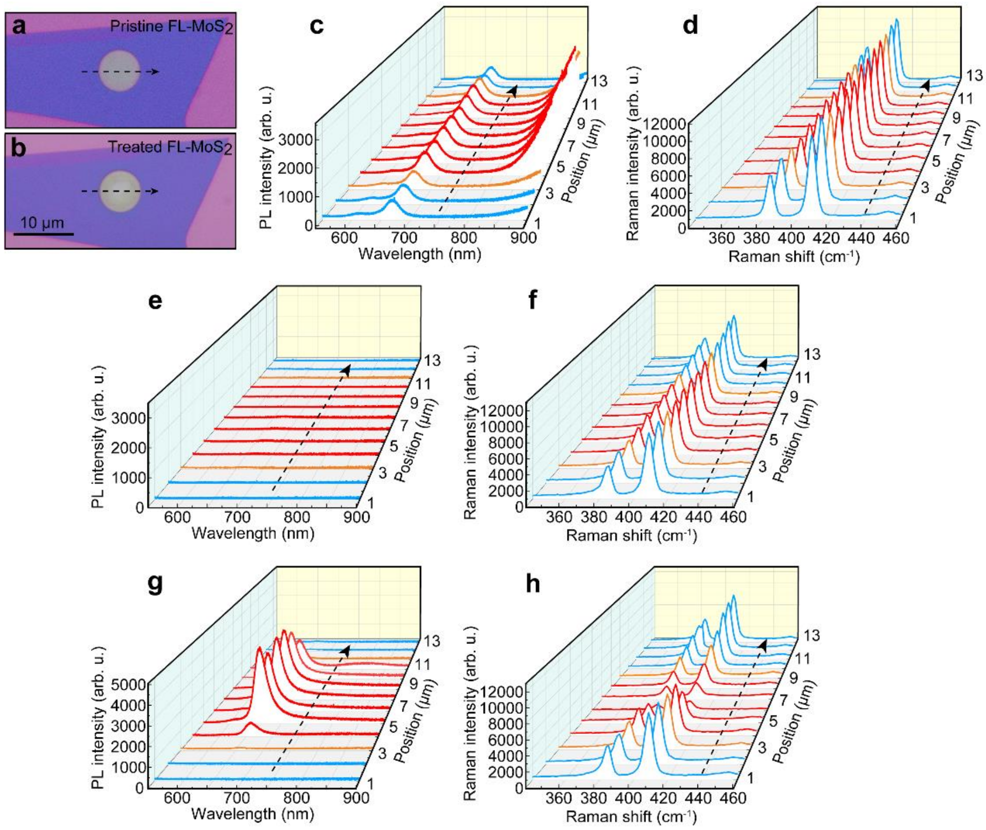

Figure S8. Optical characterizations on the few-layer MoS_2. (a, b) Optical microscopy images of few-layer MoS_2 before (a) and after (b) the plasma and laser treatments. (c, d) PL (c) and Raman (d) spectra of the pristine few-layer MoS_2 sample. (e, f) PL and Raman spectra of the plasma-treated few-layer MoS_2 sample. (g, h) PL and Raman spectra of the few-layer MoS_2 after plasma treatment followed by laser irradiation.

Table S2 Comparative summary of key parameters in plasma treatment and laser irradiation for PL modulation of MoS_2

Method	**Layer number**	**Processing parameters**	**Mechanism for PL modulation**	**Enhancement factor**	**Ref.**
O_2 plasma	1L	RF power: 5 W; Pressure: 37.5 mTorr	Healing of sulfur vacancies	~10	4
O_2 plasma	1L	RF power: 100 W; Pressure: 250 mTorr	Oxidation	quenching	5
O_2 plasma	Few-layer	RF power: 20 W; Pressure: 200 mTorr; Treated time: 3 min	Layer decoupling due to ion intercalation	~16	6
O_2 plasma	Few-layer	RF power: ~15 W; Pressure: 400 mTorr; Treated time: 3 min; DC bias: 15–20 V	Layer decoupling due to ion intercalation	~20 (4L)	7
O_2 plasma	Few-layer	RF power: 180 W; Treated time: 10 s	Shielding from a surface oxide layer	~3 (3L)	8
O_2 plasma	Few-layer	RF power: 5~30 W; Pressure: 285 mTorr; Treated time: 2 min	Layer decoupling due to ion intercalation	~20 (2L)	9
O_2 plasma	Few-layer	Plasma power: 40 W; Pressure: 1 Pa; treated time: 2–60 s	Oxidation and etching	quenching	10
O_2/Ar plasma	multilayer	Oxygen: Ar = 3:1; Pressure: ~5 mbar; Treated time: 14 s	Layer decoupling due to ion intercalation	~1.2 (4L)	11
Laser irradiation	1L	Power intensity: 4.5×10^5 W/cm^2; Wavelength: 514.5 nm, Treated time: 10 s to 25 min	Healing of sulfur vacancies	~5.5	12
Laser irradiation	1L	Power: 50 mW; Wavelength: 532 nm; Treated time: 10 s to 15 min; Under pure oxygen atmosphere	Healing of sulfur vacancies	3.8	13
Laser irradiation	1L	Power intensity: 5.8×10^5 W/cm^2; Wavelength: 532 nm; Treated time: 10 s to 25 min	Healing of sulfur vacancies	~2	14
Laser irradiation	Multi-layer	Power: 10–17mW; Wavelength: 532 nm; Treated time: 10 s to 15 min; Under pure oxygen atmosphere	Etching	/	15
Laser irradiation	Few-layer	Power: 10–40 mW; Wavelength: 532 nm; Treated time: 60 s	Etching and shielding from a surface oxide layer	~3 (4L)	16
O_2 palsma and laser irradiation	Few-layer	RF power: 5 W; Pressure: 37.5 mTorr; DC bias: 70-120 V; plasma treated time: 5 s; Laser power: ~460 μW; Treated time: 1 s	Layer decoupling	~30	Our work

References

1. Y. Huang, Y. K. Wang, H. Xin-Yu, G. H. Zhang, X. Han, Y. Yang, Y. Gao, L. Meng, Y. Wang, G. Z. Geng, L. W. Liu, L. Zhao, Z. H. Cheng, X. F. Liu, Z. F. Ren, H. X. Yang, Y. Hao, H. J. Gao, X. J. Zhou, W. Ji and Y. L. Wang, *InfoMat.*, 2021, **4**, 1–13.
2. H. Shi, R. Yan, S. Bertolazzi, J. Brivio, B. Gao, A. Kis, D. Jena, H. G. Xing and L. Huang, *ACS Nano*, 2013, **7**, 1072–1080.
3. Y. A. Romaniuk, S. Golovynskyi, A. P. Litvinchuk, D. Dong, Y. Lin, O. I. Datsenko, M. Bosi, L. Seravalli, I. S. Babichuk, V. O. Yukhymchuk, B. Li and J. Qu, *Physica E*, 2022, **136**, 114999.
4. H. Nan, Z. Wang, W. Wang, Z. Liang, Y. Lu, Q. Chen, D. He, P. Tan, F. Miao, X. Wang, J. Wang and Z. Ni, *ACS Nano*, 2014, **8**, 5738–5745.
5. N. Kang, H. P. Paudel, M. N. Leuenberger, L. Tetard and S. I. Khondaker, *J. Phys. Chem. C*, 2014, **118**, 21258–21263.
6. R. Dhall, M. R. Neupane, D. Wickramaratne, M. Mecklenburg, Z. Li, C. Moore, R. K. Lake and S. Cronin, *Adv. Mater.*, 2015, **27**, 1573–1578.
7. J. Wu, S. Li, X. Wang, Y. Huang, Y. Huang, H. Chen, J. Chen, J. She and S. Deng, *ACS Appl. Mater. Interfaces*, 2023, **15**, 58556–58565.
8. C. Pei, X. Li, H. Fan, J. Wang, H. You, P. Yang, C. Wei, S. Wang, X. Shen and H. Li, *ACS Appl. Nano Mater.*, 2020, **3**, 4218–4230.
9. L. Zhang, H. Nan, X. Zhang, Q. Liang, A. Du, Z. Ni, X. Gu, K. K. Ostrikov and S. Xiao, *Nat. Commun.*, 2020, **11**, 5960.
10. Y. Zhang, J. Liu, Y. Pan, K. Luo, J. Yu, Y. Zhang, K. Jia, H. Yin, H. Zhu, H. Tian and Z. Wu, *J. Mater. Sci.: Mater. Electron.*, 2019, **30**, 18185–18190.
11. J. Jadwiszczak, C. O'Callaghan, Y. Zhou, D. S. Fox, E. Weitz, D. Keane, C. P. Cullen, I. O'Reilly, C. Downing, A. Shmeliov, P. Maguire, J. J. Gough, C. McGuinness, M. S. Ferreira, A. L. Bradley, J. J. Boland, G. S. Duesberg, V. Nicolosi and H. Zhang, *Sci. Adv.*, 2018, **4**, eaao5031.
12. A. Bera, D. V. S. Muthu and A. K. Sood, *J. Raman Spectrosc.*, 2018, **49**, 100–105.
13. C. Hou, J. Deng, J. Guan, Q. Yang, Z. Yu, Y. Lu, Z. Xu, Z. Yao and J. Zheng, *Phys. Chem.*

Chem. Phys., 2021, **23**, 24579–24588.

14. H. M. Oh, G. H. Han, H. Kim, J. J. Bae, M. S. Jeong and Y. H. Lee, *ACS Nano*, 2016, **10**, 5230–5236.
15. A. Castellanos-Gomez, M. Barkelid, A. M. Goossens, V. E. Calado, H. S. van der Zant and G. A. Steele, *Nano Lett.*, 2012, **12**, 3187–3192.
16. J. Lu, J. H. Lu, H. Liu, B. Liu, K. X. Chan, J. Lin, W. Chen, K. P. Loh and C. H. Sow, *ACS Nano*, 2014, **8**, 6334–6343.